



Aging-induced anisotropy of mechanical properties in steel products: Implications for the measurement of engineering properties[☆]

M.D. Richards^{*}, E.S. Drexler, J.R. Fekete

National Institute of Standards and Technology, Materials Reliability Division, 325 Broadway, Boulder, CO 80305, USA

ARTICLE INFO

Article history:

Received 4 January 2011

Received in revised form 9 August 2011

Accepted 8 September 2011

Available online 16 September 2011

Keywords:

Mechanical characterization

Steel

Bulk deformation

Sheet forming

Aging

ABSTRACT

Strain aging in low-carbon steels is a well-known strengthening phenomenon, the typical results of which are an increase in yield stress and/or an increase in the extent of discontinuous yielding. Aging effects are generally characterized through the use of results from mechanical tests in which the strain path prior to aging (prestrain) and the strain path after aging are in the same direction. However, these tests do not completely characterize the properties of aged materials, since the effects of aging are reduced when materials are tested in directions different than the direction of prestrain. The result is anisotropy of properties which can affect the performance of industrial products. In this paper, the effect is demonstrated in two examples of industrial products made from low carbon steels, the aging of which during processing results in performance changes that are not predicted through standard tensile testing of as-fabricated products. The first example compares the effect of aging on yield strength and dent resistance of stamped hood panels on an electro-galvanized, Al killed, bake hardenable sheet steel for auto body panel applications. The second example shows the effect of aging on the anisotropy of tensile data from two American Petroleum Institute (API) grade X100 pipe steels in the as-received condition.

The data show that the performance gains realized from strain-aging in the tensile tests on base material are not apparent in the tensile data from the stamped panels after aging, but the dent resistance clearly demonstrated the beneficial effect of aging. The high degree of anisotropy in the yield strength and yielding behaviors between the circumferential and longitudinal tensile data in the two pipe steels demonstrates the effect of strain path on a materials response to aging, which may occur during downstream processing or in field service. The manifestation of material properties that are dependent upon the relationship between the pre-aging strain direction and the post-aging strain direction underscores the importance of correct evaluation of mechanical performance in the design of structural components in materials which undergo aging.

Published by Elsevier B.V.

1. Introduction

The process of strain aging is of considerable commercial interest due to its applicability to many types of structural components typically manufactured from steel. In the mechanical design of these components, the yield strength obtained from uniaxial tensile tests is often an important criterion for assessment of material performance and suitability for service. Strain aging can result in a significant increase in the uniaxial yield strength when the test direction is collinear with the direction of the prestrain. However, when these directions are not collinear, additional time and temperature are required to achieve equivalent aged performance [1]. Processing, fabrication and service conditions influence the

presence or absence of changes to strength induced by aging. Understanding these influences is of critical importance in determining the fitness of a component for service, as well as evaluation of the effectiveness of aging as a strengthening process.

1.1. Review of strain aging

Strain aging in steel is a strengthening mechanism where point defects, such as interstitial carbon and nitrogen atoms, within the body-centered cubic (BCC) iron lattice, interact with free dislocations, increasing their resistance to motion under an applied shear stress. The high mobility of carbon and nitrogen atoms at relatively low temperatures ($\sim 200^\circ\text{C}$) makes strain aging an industrially feasible strengthening mechanism. However, aging at room temperature can also occur, with the timeframe ranging from several months to several hours (depending on numerous factors). The Cottrell and Bilby model for strain aging [2] developed in 1949 is still seminal in describing certain aspects of the strain aging

[☆] Contribution of an agency of the U.S. government, not subject to copyright.

^{*} Corresponding author. Tel.: +1 303 497 4866; fax: +1 303 497 5030.

E-mail address: mark.richards@nist.gov (M.D. Richards).

process. When a tensile specimen is prestrained, unloaded, aged and subsequently reloaded in uniaxial tension, the stress–strain relationship of the aged specimen exhibits some typical characteristics [1,3–6]:

- A rapid return of the sharp yield point, accompanied by an upper yield stress and a load drop to a lower yield stress that is greater than the flow stress at the point of unloading during prestraining;
- A return of discontinuous yielding and yield point elongation (YPE);
- Depending upon numerous factors, an increased strain hardening rate, increased tensile strength and decreased total elongation.

The effectiveness of strain aging, as it is measured during loading in a given direction, is highly influenced by the degree of collinearity of that loading with the prestrain path. Typically, strain aging is characterized under conditions for which the pre- and post-aging strain paths are collinear and in the same direction. Situations in which the strain path of the prestrain and post-aging deformations is significantly different require a deeper level of understanding and care in the approach to determining yield strength, in order to ensure that appropriate mechanical properties are employed for engineering applications.

In the extreme case, the direction of post-aging deformation is aligned, but reversed from that of prestraining, as is the case during a test to evaluate the Bauschinger effect [7]. The significant implications of material flow behavior under strain reversal are the loss of a distinct transition between elastic and plastic deformation, typically termed a “sharp” yield point, and greatly diminished flow stress in the reverse direction, as compared with the original direction of strain. The decreased flow stress in the reversed direction has been attributed to the reversed motion of large groups of dislocations [8] due to short-range dislocation phenomenon and long-range internal stresses, typically caused by dislocation pile-ups that assist reversed dislocation motion [9–16]. Richards et al. [17] evaluated the *in situ* Bauschinger effect of three medium carbon steels from room temperature up to temperatures in which dynamic strain aging is effective. They found that while the aging mechanisms significantly improve the resistance to strain reversal at elevated temperature, the materials still exhibited reduced reversed flow stress values than those exhibited at the same accumulated strain in uniaxial tension and very soft yielding behavior. Similar results for static strain aging were demonstrated by Aran and Demirkol [9].

In situations where the prestrain path and post-aging deformation are not aligned, the combination of strain aging effect and Bauschinger effect (due to residual elastic lattice strains) complicates characterization of final material properties. Microstructural factors can also influence the effect of strain path on effectiveness of the strain aging process. For example, Wilson and Ogram [18] performed experiments on steel plates with grain sizes between $50 \text{ grains} \times \text{mm}^{-2}$ and $3900 \text{ grains} \times \text{mm}^{-2}$, where the post-aging deformation was transverse to the prestrain orientation. These investigators showed that after a tensile prestrain along the longitudinal direction, the effect of aging on the return of the YPE in tensile specimens taken transverse to the prestrain direction depended upon the grain size. Ultrafine and fine-grained materials achieved a return of YPE and sharp yield point in 100 min to 300 min, respectively, at 89°C , whereas the coarse-grained material exhibited no return of the YPE even after 10^5 min at 89°C , as opposed to approximately 10 min for the case in which the prestrain and post aging strain paths were collinear [18]. Wilson and Ogram [18] achieved similar results from reversed torsion Bauschinger effect tests by use of coarse and fine grain sized low carbon steel tube. Wilson and Ogram [18] suggested that grain

boundaries are sites of high dislocation density, and in coarse-grained materials the time delay for sufficient solute diffusion from the grain interior to saturate dislocations in the grain-boundary region is prohibitively long. Differences in post-aging yielding behavior in the aligned and non-aligned conditions with respect to the prestrain condition may be caused by the operability of different dislocation sources for each situation. For the non-aligned case, the dislocations required for the accommodation of plastic deformation are generated from grain boundaries instead of the grain core as in the aligned case, grain boundaries have significantly higher dislocation densities and the time required for sufficient solute segregation from the grain core to the boundary region to fully pin the dislocations there is significantly longer. Therefore the strain energy required to generate dislocations from the grain boundaries is much lower than that for the fully pinned grain core. The directional aspects of the strain aging process can reduce the reliability of tensile test measurements to accurately characterize material properties under complex loading conditions.

Certain steelmaking processes take advantage of the directional nature of aging behavior. The most well known of these is temper rolling which, through the suppression of the return of YPE and therefore the formation of Lüders bands¹, results in improved surface quality in stamped steel parts. The significance of temper rolling was shown by Tardif and Ball [19], who compared the effect of aging on the return of YPE on a low-carbon sheet steel that had been either prestrained in tension or temper rolled. Temper rolling, followed by tensile loading along the rolling direction after aging, lengthened the time period required for the return of the yield point by over 2 orders of magnitude compared to that for tensile prestrain and tensile post-aging loadings. The complex deformation induced during temper rolling was of sufficient misalignment to the post-aging deformation to realize the delayed response to aging. Additional temper-rolled specimens were prestrained in tension by a given amount, aged for various periods and subsequently tested in tension. As the tensile prestrain increased from 0.25% to 2.0%, the delay in the return of YPE diminished and exhibited behavior similar to that for a prestrained sheet as opposed to a temper-rolled sheet without prestrain. Elliot et al. [20] observed similar results for fully reversed torsion. Thus, even small levels of deformation are sufficient to decay the dislocation structure and residual lattice strains formed during temper-rolling and become reformed and aligned with the most recent strain path. Jeong [21] observed similar results comparing results from tensile tests on low carbon sheet steel in the tensile prestrained condition and in stamped door panels, where the strength increase exhibited in the tensile prestrain condition was not exhibited in the stamped door panels after aging for 17 days.

The nature of the metallurgy and processing of pipeline steel results in their susceptibility to strain aging [22,23]. Plastic strains are introduced during the forming process in the circumferential orientation, the extent of which is dependent on the diameter, thickness, through thickness microstructural variations in the base-plate due to thermo-mechanical processing and accelerated cooling practices, and yield strength of the material. Aging can be introduced in a pipe during the period at which it is at elevated temperature during the coating process, during welding, while the

¹ In an aged material, such as an annealed, low-carbon steel, yielding typically occurs within a localized deformation band in the reduced gauge section of the test piece, typically accompanied by a sharp drop in applied load. Deformation proceeds through propagation of distinct bands of intense plastic deformation, called Lüders bands. Lüders bands propagate in a staggered, discontinuous manner during which the applied force remains essentially constant in magnitude with small fluctuations. This can result in a series of ridges on a stamped steel part, which is detrimental to the surface uniformity.

pipe section is exposed to the environment awaiting installation, or during long service periods. The effects of strain-aging can be of particular concern with high-strength pipeline steels, as the increase in yield strength is usually accompanied by a loss in uniform elongation (ϵ_u) and strain-hardening capacity, which results in a yield strength to tensile strength ratio that approaches a value of 1.

In some applications, the effects of aging processes on the mechanical properties are considered to be undesirable [24]. Recent research on American Petroleum Institute (API) X100 grade pipeline steels formed through the UOE process [25,26] showed a distinct difference between the longitudinal and transverse tensile yielding behaviors. It was shown that the yield behavior in a direction longitudinal to the pipe axis exhibited a gradual transition from elastic to plastic deformation, with a low elastic limit. The 0.2% offset yield strength values were 689 MPa [25] and 678 MPa [26] respectively. In contrast, as-machined, hoop direction tensile specimens exhibited a substantially higher elastic limit along with a distinct transition from elastic to plastic deformation; the 0.2% offset yield strength levels were 775 MPa [25] and 774 MPa [26], a difference of approximately 100 MPa in yield strength as compared with the longitudinal direction. Furthermore, Li et al. [25] showed that after aging for 1 h at 180 °C the longitudinal tensile data exhibited a small increase in yield strength and elastic limit, but maintained a yielding behavior characteristic of continuous yielding. Whereas, the transverse data, which exhibited a distinct yield point in the as-fabricated condition, demonstrated an upper yield point and load drop followed by discontinuous yielding after 5 min of aging at 180 °C. Similar results were shown by Duan et al. [26]. Other research [27] has demonstrated for X80 pipe that the longitudinal and transverse directions will exhibit distinct yielding behavior in the aged condition.

Because the directional nature of aging can result in mechanical properties that are directionally dependent (anisotropic), strain aging can produce unexpected mechanical behavior in certain situations. The balance of this paper will describe two examples of the influence of the non-isotropic strengthening induced by strain aging on the properties of engineering materials, showing that if strain aging is a component of the processing of a material, whether intentional or not, its mechanical properties must be carefully characterized to ensure they are completely understood for design purposes. In the first example, tensile testing is shown to not always accurately predict the dent resistance in an automotive sheet steel. In the second, process-induced deformation and strain aging combine to induce significant differences in the longitudinal vs. transverse tensile properties in a high-strength pipeline steel, with implications for pipeline design methods.

2. Example 1: Effect of strain aging on the strength and dent resistance of automotive body panels

The ability to resist denting from incidental contact is an important performance characteristic of automotive exterior body panels. Standard tests have been developed to evaluate the resistance of body panels to denting forces, and the relationship between material and geometry parameters and dent resistance has been described by the following expression [28–30]:

$$\text{Dent resistance} = K \times \text{YS} \times t^n \quad (1)$$

where dent resistance is the force to create a dent of fixed depth, YS is yield strength, t is panel thickness, and n and K are empirical constants related to the panel stiffness and the range for n is between 2.3 and 2.4 [28]. It is apparent from this equation that increased YS should result in increased dent resistance. The increase in YS resulting from strengthening by strain-aging of low-carbon steels has been used to improve exterior-panel dent resistance since the

Table 1
Chemical analysis of tested material.

| Element | C | Mn | P | S | Al | Si | Cu |
|-------------------|------|------|-------|-------|-------|------|------|
| Mass fraction (%) | 0.02 | 0.17 | 0.055 | 0.008 | 0.041 | 0.01 | 0.01 |

Table 2

Mechanical properties of tested materials, as received from supplier and after pre-strain and aging per SAE J2340, which was 30 min aging period at 175 °C following a 2% prestrain.

| Condition | YS _{0.2%} Offset (MPa) | |
|-------------|---------------------------------|-------|
| | Long | Trans |
| As received | 230 | 240 |
| Strain-aged | 300 | 300 |

early 1990s. Today, many parts are in production with these materials, which are known as BH or “bake hardenable” steels. The strain required to develop significant strain aging is induced in the stamping process used to form the panels into the final shape, with the aging, or “baking”, occurring in the paint bake ovens during body manufacturing.

Based on the above equation, in a given location on a panel, non-strain-aged steels should give dent resistance equivalent to that of strain-aged steels if the yield strength and thickness in the panel are the same. However, evaluation of dent resistance before and after a simulated paint-bake thermal cycle shows that although the effect of aging is not apparent from tensile testing of hood material, its presence contributes significantly to the dent resistance of the panels. The behavior is demonstrated in the following example, through comparison of mechanical properties from uni-axial tensile tests and evaluation of dent resistance.

2.1. Experimental

A production hood outer panel was used in the present example. The material used for the hood panel was a commercially available electro-galvanized, Al killed, bake hardenable steel with a minimum yield strength of 210 MPa and a minimum thickness $t=0.70$ mm (actual thickness in the panels ranged from 0.71 mm to 0.73 mm). Chemical analysis of the base metal and mechanical properties was provided by the steel supplier, and is listed in Tables 1 and 2, respectively. Hood panels were pressed and assembled in production plants. The strain level in the hoods was measured in an area close to the cowl (location “A” in Fig. 1). The strain in this area was biaxial with a nominal value of $2\% \times 1\%$. The hoods were acquired at the body shop in the assembly plant immediately after assembly of the outer panel to the hood inner panel, but prior to the paint operation. Half of the hoods were aged with a thermal cycle based on the characteristics of the paint operation.

Samples approximately 305 mm \times 305 mm were taken from the left center and right sides of the hood outer panel, for mechanical-property testing². Longitudinal and transverse tests were made from samples before and after aging³, the results of which are listed in Table 3. Other hoods were used for dent testing. The dent resistance testing was performed by use of the procedures found in SAE J2575⁴. The dent measurement used was the load required to create a 0.06 mm dent. The dent-testing locations are shown in Fig. 1.

² The “left” sample was at Location A in Fig. 1. The “right” sample was at the equivalent position on the right side of the hood. The “center” sample was taken at the hood centerline, at the same distance from the rear edge of the hood.

³ The longitudinal direction of the steel sheet was parallel to the centerline of the hood.

⁴ Also known as the Auto/Steel Partnership quasi-static dent test procedure.

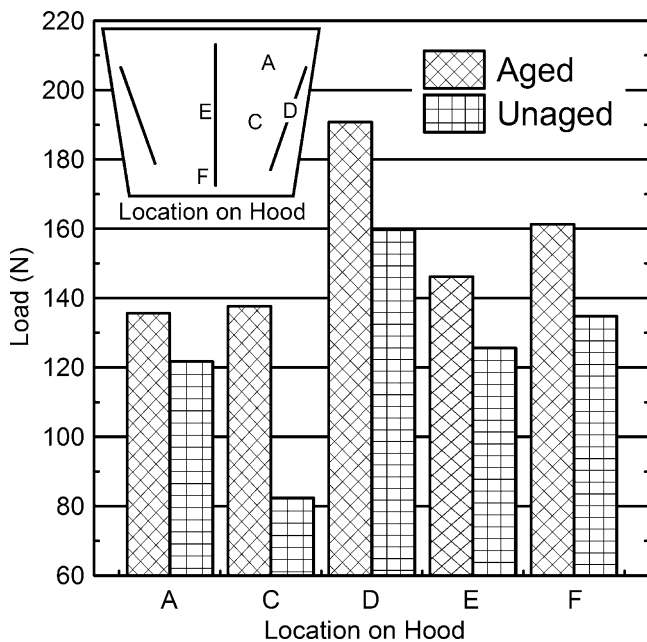


Fig. 1. Dent testing results of the load required to introduce a 0.06 mm dent from assembled hoods before and after aging.

2.2. Results and discussion

A comparison of the properties in Tables 2 and 3 shows first that there was a higher yield strength in the unaged hood panels as compared with the base-material properties in Table 2, resulting from the work hardening caused by the forming strain. The yield strength of the unaged panels was even higher than the yield strength measured after the strain aging treatment in the base material. This was evidence of the significant work hardening caused by biaxial prestrain during the forming operation on the yield strength in the formed panels. Second, the yield strength of the hood panels after aging was similar or lower than that in the panels before aging. In contrast, the base material listed in Table 2 showed the expected increase in yield strength after straining and aging. On the surface this was a puzzling result, because most literature states that the positive effect of bake hardening on dent resistance was due to the increase in yield stress.

This apparently anomalous behavior has been observed previously [30] and is another example of anisotropy induced through strain aging. The prestrain in the samples taken from assembled hoods was not uniaxial, and an increase in strength from strain aging was not observed in uniaxial tensile tests. It has been previously shown that if a biaxially prestrained sample was aged and then plastically strained along the same biaxial strain path, that an increase in the yield strength and the return of yield point typical of strain aging was observed [31]. Thus, the ability to measure an increase in strength from strain aging depends upon the method and direction of testing.

Table 3

Yield strength before and after aging cycle, sampled from areas in the left, center and right of the hood.

| Condition | YS _{0.2% Offset} (MPa) | | | | | |
|-----------|---------------------------------|-------|--------|-------|-------|-------|
| | Left | | Center | | Right | |
| | Long | Trans | Long | Trans | Long | Trans |
| Unaged | 327 | 323 | 340 | 366 | 349 | 369 |
| Aged | 323 | 319 | 321 | 318 | 321 | 307 |

Fig. 1 shows the load required to cause a 0.06 mm dent for the aged and unaged conditions for dent tests performed at numerous locations about the hood panel. Fig. 1 shows that in all cases, the dent resistance of the aged hoods is higher than that of the unaged hoods, even though the material thickness is the same and the panel yield strength is the same or lower. Denting forces result in multi-axial out-of-plane bending in the panel, which results in a strain path much more similar to the biaxial straining than that resulting from a tensile test. The improved dent resistance in the hoods indicates that strain aging is an effective strengthener in this case, even though tensile results do not show a strength increase and therefore do not indicate an increased dent resistance based upon the predictive equation.

Another possible factor that could affect dent resistance is the reduction in stiffness near the yield strength of non-strain-aged material as compared to a strain-aged material of the same macroscopic yield strength. This is caused by microyielding in the non-strain-aged material due to a deviation from the proportional limit, the limit in which the stress–strain curve deviates from linearity. In a non-strain-aged material that exhibits a gradual transition between elastic to plastic deformation, the proportional limit can be much lower than commonly used engineering criteria such as the offset yield stress. In aged materials, where dislocations are pinned by interstitial solute atmospheres, the transition from elastic to plastic deformation is distinct and typically accompanied by a drop in strength to the offset yield strength. Therefore the measured stiffness for non-strain aged parts would be less than that realized in aged materials when the stiffness is measured at a stress level near the offset yield stress. Because dent resistance is related to stiffness, as shown in the predictive equation, improved dent resistance would be expected when BH steels are used.

2.3. Conclusions for Example 1

These results show that BH steels strained biaxially before aging exhibit a positive increase in dent resistance after aging even when no increase in yield strength is observed in a uniaxial tensile test. The additional increment in dent resistance is caused by the increase in strength from aging the biaxially pre-strained hood which is not evident in simple tensile tests of specimens sectioned from the aged hood. These results would not be predicted from the dent resistance equation based upon tensile properties of the aged and unaged hoods. Thus, decisions on material selection for panels that have requirements for dent resistance should be influenced more by actual dent-resistance results than by tensile-test results.

3. Example 2: Effect of strain aging on mechanical properties of high-strength pipeline steels

The traditional stress-based pipeline design approach has treated pipelines as extended pressure vessels where the design limits the applied stress and strain to the elastic regime and the strain hardening capacity is treated as a safety factor in design. Strain-based design, which extends the performance limits to permit a certain amount of plastic strain, is becoming the preferred design approach for use with high strength materials with limited strain hardening capacity and in areas in which the pipeline may be subjected to high longitudinal deformation, such as seismic activity, frost heave and landslides [32,33].

The typical loading of a pressurized gas transmission line is in the hoop direction; therefore in order to maintain pressure containment in service, the mechanical properties in the circumferential direction are of great interest to pipeline designers. The longitudinal strain capacity, in addition to the circumferential yield strength, is used as a limit state and as a measure of the safety factor in

strain-based design [34]. Mechanical property based performance limits for pipeline design, require proper codes and standards for the accurate and repeatable measurement of characteristic mechanical behavior, as well as the development of science behind factors which alter the behavior outside of traditional theory.

The pipeline community faces challenges in the implementation of advanced high strength materials and strain-based design methodologies. A better understanding of the anisotropy of material deformation behavior and how it is influenced by forming strains and the aging phenomena will result in better models and reduced uncertainty. This study compares the tensile properties of two experimental API grade X100 pipelines in the longitudinal and circumferential orientations to ascertain the effects of strain aging on the strength and strain capacity of these pipe materials.

3.1. UOE-forming

UOE forming is a common method for producing pipeline sections from steel plate. The process takes discrete plate and forms it into a cylinder that is closed with a seam weld [35]. Plastic strains are introduced when (1) the edges of the plate are crimped for welding, (2) during the “U” forming step when the plate is pressed into a U shape, (3) during the “O” forming step when the crimped edges are brought together, and (4) during the “E” forming step when a mechanical expansion is employed to reshape the pipe to within circular tolerances.

Strains introduced during the UOE process are almost entirely transverse in nature. The amount of strain introduced during each step is dependent on the thickness of the plate material and the diameter of the pipe [36], as well as the yield strength of the plate. For example, strains introduced from the mechanical expansion may be 1% or more [36,37]. Also, variations exist in the amount of strain introduced, depending on the position sampled around the circumference of the cylinder. These factors all have an influence in the magnitude of strain aging found in the transverse direction of the final pipe section. Significant strain aging results in anisotropy of mechanical properties, as described in the study below.

3.2. Experimental

Tensile tests were conducted on material from two experimental linepipes of API X100 grade steel (X100 refers to the minimum yield strength in ksi). The pipe sections, supplied by two different manufacturers, are low-carbon steels strengthened through microalloying and TMCP (thermo-mechanical control processing), and are referred to as pipe A and pipe B. Fig. 2 shows scanning electron micrographs of the X100 pipe A (Fig. 2a) and X100 pipe B (Fig. 2b) in the longitudinal direction taken midway between the centerline and the surface. The SEM micrographs in Fig. 2 show that each material is composed of a granular bainitic structure with the pipe B material in Fig. 2b exhibiting regions of elongated sheaves of bainitic ferrite and aligned second phase carbides. Each was made into pipe with a diameter of 1.2 m and thickness of 21 mm through the use of forming and welding techniques similar to those found in UOE-formed linepipes now in service. The chemistries for pipe A and pipe B are listed in Table 4. It is shown in Table 4 that pipe A has higher C and microalloying (V, Nb, Ti) content and substantially more Cr which is primarily used to improve hardenability.

The pipe sections were received in the as-formed condition from the pipe mill without undergoing the typical thermal treatment from the fusion bonded epoxy (FBE) coating process. The materials underwent aging in the ambient environment during the summer months in which pipe temperatures could exceed 50 °C during the day and 25 °C at night. The following relationship [38] was used to approximate an equivalent aging period at the typical 200 °C FBE

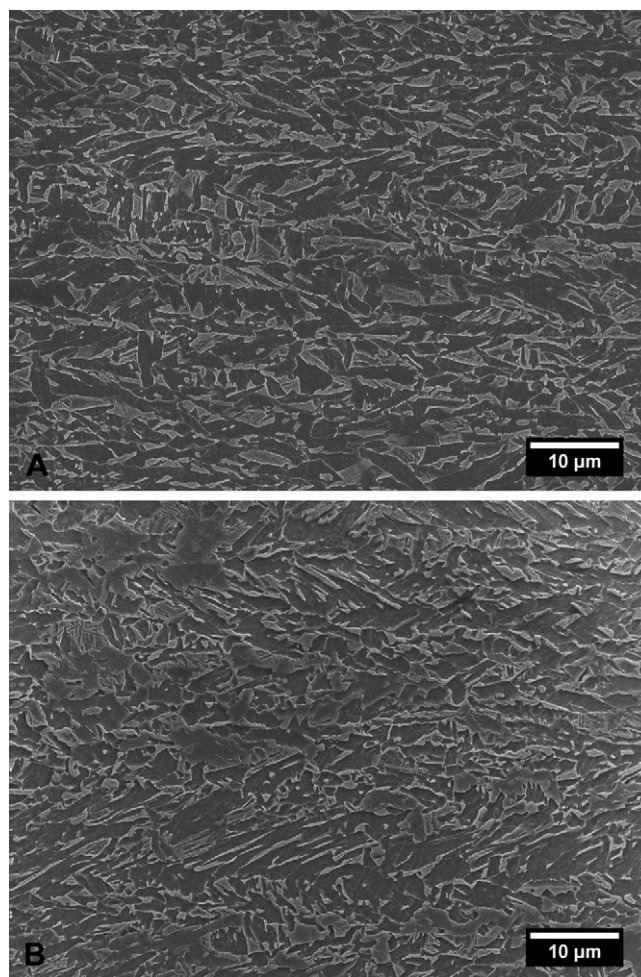


Fig. 2. Scanning electron micrograph images of the plane longitudinal to the pipe axis and rolling direction of pipe A (a) and pipe B (b), nital etch.

process using established diffusivity constants for carbon in iron [39]

$$\bar{x} \cong \sqrt{Dt} \quad (2)$$

where x is the mean diffusion distance, D is the diffusivity of carbon in iron and t is the time period. The combined diffusion distance at the daytime and nighttime temperatures over a 4-month period is equivalent to a 5 min period at the typical FBE coating process temperature, which is typical of most FBE coating times.

Round tensile specimens were machined according to ASTM E8-01 directly from the curved pipe material for both the longitudinal and circumferential orientation tests. Unflattened, round tensile specimens, which are machined out of the curved pipe, do not evaluate the full thickness of the pipe, unavoidably sampling over a microstructural and strain history gradient. However, it has been shown that unflattened, round tensile specimens provide a

Table 4
Chemical composition of the pipe materials in mass fraction (%).

| Alloy | C | Mn | Ni | Cr | Cu | Si | S |
|--------|-------|------|-------|-------|-------|------|-------|
| Pipe A | 0.076 | 1.73 | 0.28 | 0.200 | 0.15 | 0.30 | 0.007 |
| Pipe B | 0.061 | 1.75 | 0.49 | 0.030 | 0.29 | 0.10 | 0.007 |
| Alloy | P | Mo | V | Nb | Ti | Al | N |
| Pipe A | 0.010 | 0.22 | 0.006 | 0.045 | 0.016 | 0.03 | 0.007 |
| Pipe B | 0.005 | 0.30 | 0.004 | 0.026 | 0.009 | 0.03 | 0.007 |

Table 5

Tensile mechanical property data from pipes A and B, including common definitions for yield strength, upper yield point (UYP), lower yield point (LYP) and 0.2% offset and the associated standard deviations (SD) in the measured mechanical property.

| Mechanical property | Pipe A | | | | | | Pipe B | | | | | |
|------------------------------------|--------|-------|-------|-------|-------|-------|--------|-------|-------|-------|-------|-------|
| Test | 1 | 2 | 3 | 4 | Mean | SD | 1 | 2 | 3 | 4 | Mean | SD |
| Longitudinal orientation | | | | | | | | | | | | |
| YS _{0.2% offset} (MPa) | 713 | 725 | 721 | 730 | 722 | 6.9 | 728 | 735 | 720 | 734 | 729 | 7.0 |
| UTS (MPa) | 842 | 865 | 845 | 866 | 855 | 12.8 | 844 | 846 | 828 | 834 | 838 | 8.4 |
| $\epsilon_{\text{Uniform}}$ | 0.051 | 0.045 | 0.048 | 0.042 | 0.046 | 0.004 | 0.061 | 0.055 | 0.056 | 0.060 | 0.058 | 0.003 |
| ϵ_{Final} | 0.168 | 0.199 | 0.229 | 0.209 | 0.201 | 0.026 | 0.205 | 0.210 | 0.220 | 0.214 | 0.212 | 0.006 |
| Y/T (0.2% offset) | 0.847 | 0.837 | 0.853 | 0.842 | 0.845 | 0.007 | 0.863 | 0.869 | 0.869 | 0.880 | 0.870 | 0.007 |
| Circumferential orientation | | | | | | | | | | | | |
| UYP (MPa) | 925 | 939 | 939 | 938 | 935 | 7.0 | 846 | 865 | 861 | 864 | 859 | 8.9 |
| LYP (MPa) | 900 | 911 | 908 | 907 | 907 | 4.5 | 823 | 834 | 826 | 837 | 830 | 6.4 |
| YS _{0.2% offset} (MPa) | 902 | 920 | 916 | 909 | 912 | 8.0 | 831 | 835 | 827 | 838 | 833 | 4.8 |
| UTS (MPa) | 911 | 921 | 916 | 917 | 916 | 3.9 | 864 | 871 | 862 | 876 | 868 | 6.2 |
| $\epsilon_{\text{Uniform}}$ | 0.017 | 0.040 | 0.027 | 0.022 | 0.026 | 0.010 | 0.041 | 0.048 | 0.043 | 0.056 | 0.047 | 0.007 |
| ϵ_{Final} | 0.152 | 0.193 | 0.190 | 0.170 | 0.176 | 0.019 | 0.074 | 0.169 | 0.180 | 0.174 | 0.174 | 0.006 |
| Y/T (0.2% offset) | 0.990 | 1.000 | 1.000 | 0.991 | 0.995 | 0.005 | 0.962 | 0.959 | 0.958 | 0.956 | 0.959 | 0.002 |
| Y/T (UYP) | 1.015 | 1.020 | 1.025 | 1.022 | 1.021 | 0.004 | 0.979 | 0.993 | 0.998 | 0.986 | 0.989 | 0.008 |

closer representation of material flow behavior in the yield regime compared to flattened strap specimens (which tend to exhibit a depressed yield response due to the Bauschinger effect [40]), when ring expansion tests are used as the basis for comparison as being the most representative of the material behavior [40,41]. The material for the tensile tests was sectioned from the 9 o'clock position with respect to the seam weld located at 12 o'clock. The specimens were tested on a 250 kN force capacity servo-hydraulic load frame at a constant engineering strain rate of $6.5 \times 10^{-5} \text{ s}^{-1}$ at room temperature. The test matrix comprises the two different pipeline steels, tested in both longitudinal and circumferential orientations. Four specimens with a gauge diameter of 12.7 mm and gauge length of 51 mm were used for both the longitudinal and circumferential directions, for both pipes A and B, in order to sample the maximum volume through the thickness of the pipe wall.

3.3. Results and discussion

Fig. 3 shows typical stress–strain curves for both orientations from each X100 pipeline material. In the circumferential orientation both materials exhibited upper and lower yield points, followed by discontinuous yielding, characteristics of a steel material in the aged condition, and exhibited little strain hardening up to the point of instability. The longitudinal orientation exhibited a gradual transition from elastic to plastic deformation with much lower elastic limit and yield stress values and much higher strain hardening rates as compared to the circumferential orientation. For the purposes of describing these data, the ultimate tensile strength (UTS) is defined as the largest stress subsequent to yielding. As seen in Fig. 3, tests from both materials and orientations resulted in similar elongation to failure values. The uniform elongation ($\epsilon_{\text{Uniform}}$), however, was substantially lower in the circumferential direction, particularly in pipe A. Table 5 lists the tabulated tensile test data, and shows that the uniform elongation was 75% higher in the longitudinal orientation as compared with that for the circumferential orientation for pipe A; the difference was 23% for pipe B. The elongation to failure (ϵ_{Total}), however, was only about 14% higher in the longitudinal orientation for pipe A and 22% higher for pipe B.

The yield strength data are reported as the upper yield point (UYP), lower yield point (LYP), and 0.2% offset flow stress for the purpose of comparison in Table 5. All tests from both pipes met or exceeded the minimum strength requirements for the X100 grade. All definitions show that the average yield strength values were higher in pipe A than pipe B in the circumferential orientation, and higher in pipe B than in pipe A in the longitudinal orientation. The UTS was higher in pipe A than pipe B for both orientations. The higher strength exhibited by pipe A in the longitudinal

and circumferential directions are attributable to the higher C and microalloying (V, Nb and Ti) content as well as the higher Cr content in the steel.

The strength differences between the longitudinal and circumferential directions in the two pipe materials are further illustrated in Fig. 4, which shows a bar chart of the YS and UTS data for pipes A and B in the longitudinal and circumferential directions. Fig. 5 shows the ratio of the yield strength to the ultimate tensile strength (Y/T) determined from both the 0.2% offset and the upper yield point (UYP) values for YS. The difference in the YS and UTS levels in Figs. 4 and 5 both illustrate the magnitude of work hardening that occurs in the longitudinal orientation for both pipes. Figs. 4 and 5 also show similar magnitude between the values of YS and UTS

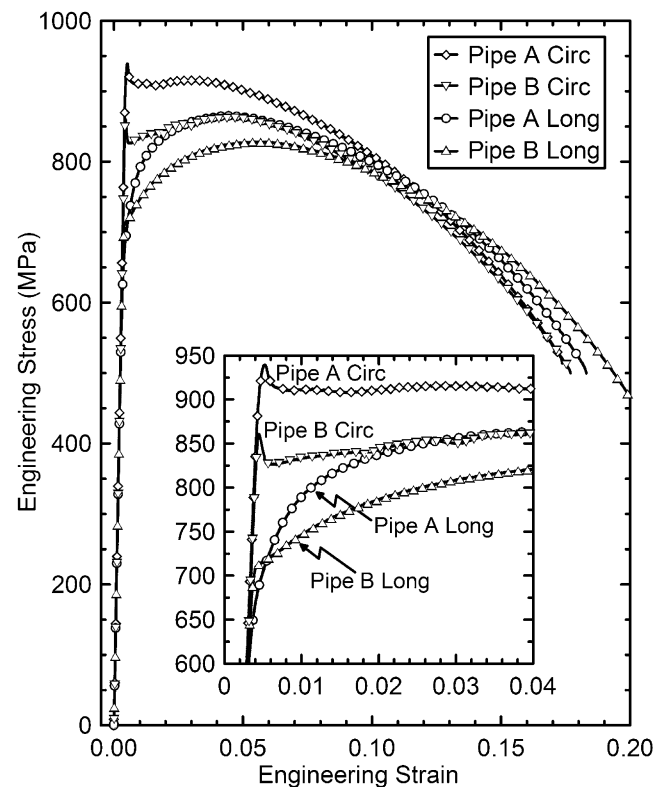


Fig. 3. Typical engineering stress versus engineering strain data from specimens sectioned from pipes A and B in the as-received condition in the longitudinal (long) and circumferential (circ) orientations, the inset shows a close-up of the low strain region to highlight the differences in yield characteristics.

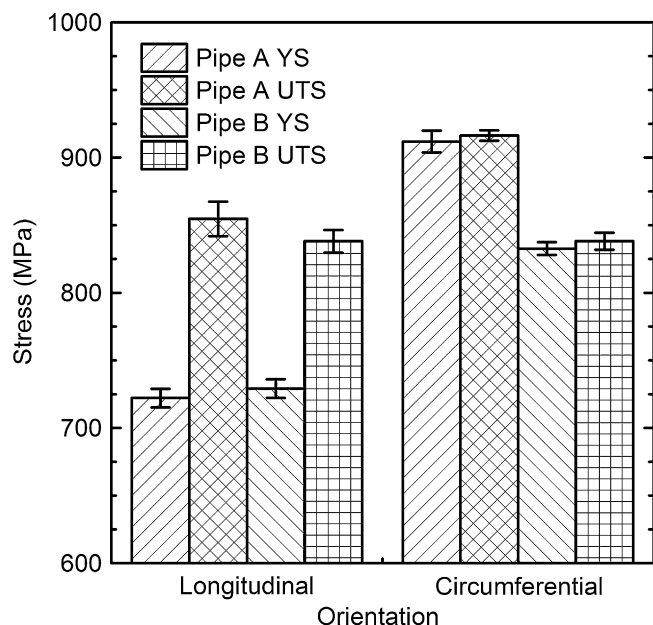


Fig. 4. Comparison of yield and ultimate tensile strength data from pipes A and B in the longitudinal and circumferential orientations. The bars indicate the standard deviation in the measured mechanical property.

in the circumferential orientations, an indication of the effects of strain aging in the circumferential direction in these materials. Materials that exhibit yield to tensile strength ratios that approach or exceed a value of 1 demonstrate negligible strain hardening. Improved understanding of the effects of strain aging and its impact on high strength materials with limited strain hardening capacities will improve the quality of stress and strain-based designs and allow for more efficient use of material with no compromise in factors of safety.

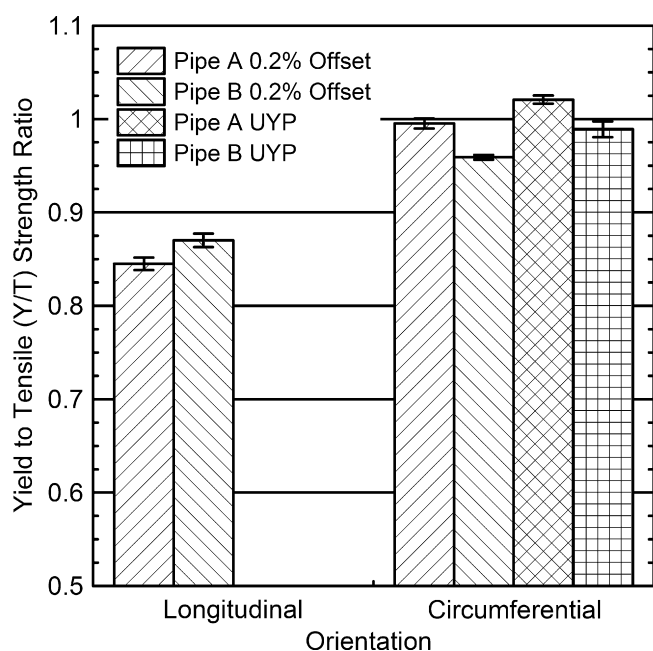


Fig. 5. Comparison of yield-to-tensile strength ratios for pipes A and B in the longitudinal and circumferential orientations using 0.2% offset and UYP values for yield strength. A specimen with a ratio of >1.0 has a yield strength greater than tensile strength. The bars indicate the standard deviation in the measured mechanical property.

3.4. Conclusions for Example 2

Comparison of the tensile properties of the two X100 materials shows the UOE process-induced anisotropy in the yield strength levels between the longitudinal and circumferential directions as shown in the literature [25,26]. Behavior apparently unique to this generation of X100 was also observed, including extremely high Y/T ratio and yield strength anisotropy in the circumferential direction for pipe A. Both pipe materials exhibited effects of strain aging in the circumferential orientation, the orientation of the last deformation step during the forming process, as demonstrated by the characteristics of yielding behavior, higher YS, and reduced uniform elongation and elongation to failure data. Of particular concern is the lack of strain hardening in Pipe A in the circumferential orientation, as the circumferential mechanical properties are what maintains pressure containment and are used to establish operational limits, and the strain hardening capacity represents additional safety factor in the design. Although the UYP is extremely high (>900 MPa), margins for safety must take into account that $UYP \approx UTS$.

4. Summary

The two examples described above demonstrate how anisotropic mechanical properties in engineered structures can be induced through non-isotropic strengthening processes such as strain aging. This occurs because processing of these materials induces specific strain paths, which in turn can result in increases in strength induced by strain aging when subsequently loaded in those same directions. Strength measured in other directions may not show the effect of strain aging or its occurrence may be delayed until after the material experiences a suitable combination of temperature and time. In the case of dent resistance of stamped automotive body panels, strain aging improves the resistance of the material to out-of-plane deformation as occurs in denting. This improvement is not exhibited in conventional tensile tests. In the case of UOE formed pipeline, the transverse strains from the expansion stage of pipe forming can result in aging-induced increases in strength and reductions in elongation in the circumferential direction that are not observed when testing in the longitudinal direction. It is shown that while the circumferential data exhibit yielding behavior characteristic of aged materials, the longitudinal data exhibits continuous yielding. This behavior is caused by the effectiveness of aging in the circumferential direction due to the previous deformation step being collinear and in the same direction as the tensile tests. In contrast, the longitudinal direction exhibits no aging because of the difference in strain path between the forming strain and testing strain directions.

These examples underscore the importance of careful testing of prototype components after processing is completed, especially if cold working followed by aging is an aspect of the process. Neither kinematic nor isotropic hardening models, as typically implemented in finite-element modeling, account for strengthening through aging in the calculations of the yield surfaces used to model forming processes. In addition, typical finite-element modeling makes no allowance for the relationship between the magnitude of the strain-aging effect and the time and temperature experienced by a component after straining. Thus, with current modeling technology, the aging effects demonstrated here can be observed only experimentally; modeling will not elucidate them. Errors can be made in both directions; components or materials may be rejected due to a failure to meet engineering requirements, or they may be over engineered if strain aging benefits the structure, as in the example of dent resistance described above.

These examples also provide encouragement to researchers to further explore this effective and efficient method of strengthening steel materials. Although the basic mechanisms are well understood, for the most part, their implementation in modeling tools is in its infancy. The less well-understood effects of nonlinearity of pre-aging and post-aging strains, and of pre-aging strain caused by multiaxial loading on post-aging behavior, will require significant additional experimental work to aid in the effective implementation of aging effects in finite element models.

Acknowledgements

The authors gratefully acknowledge General Motors Company for permission to publish data contained in the “Effect Of Age Hardening On Strength And Dent Resistance Of Automotive Body Panels” section and Dr. Nicholas Barbosa at NIST for his assistance with the SEM images. The work for the section entitled “Effect of Strain Aging on Mechanical Properties of High-Strength Pipeline Steels” was carried out under U.S. DOT contract no. DTPH56-06-X-000029 “Prj. #205”.

References

- [1] J.D. Baird, *Metal Rev.* 16 (1971) 1–18.
- [2] A.H. Cottrell, B.A. Bilby, *Proc. Phys. Soc. London A* 62 (1949) 49–62.
- [3] J.D. Baird, *Iron Steel* 36 (1963) 186–192.
- [4] J.D. Baird, *Iron Steel* 36 (1963) 326–334.
- [5] J.D. Baird, *Iron Steel* 36 (1963) 368–374.
- [6] J.D. Baird, *Iron Steel* 36 (1963) 400–405.
- [7] J. Bauschinger, *Civilingenieur* 27 (1881) 289.
- [8] R.C. Daniel, G.T. Horne, *Metall. Trans.* 2 (1971) 1161–1172.
- [9] A. Aran, M. Demirkol, *Mater. Sci. Eng.* 47 (1981) 89–92.
- [10] A. Goel, R.K. Ray, G.S. Murty, *Scr. Metall.* 17 (1983) 375–380.
- [11] R.E. Stoltz, R.M. Pelloux, *Metall. Trans. A* 7A (1976) 1295–1306.
- [12] Y.M. Yaman, A. Özsoy, K. Taşci, *J. Mater. Sci. Lett.* 9 (1990) 429–431.
- [13] A. Abel, R.K. Ham, *Acta Metall.* 14 (1966) 1489–1494.
- [14] D.V. Wilson, *Acta Metall.* 13 (1965) 807–814.
- [15] J.C. Fisher, E.W. Hart, R.H. Pry, *Acta Metall.* 1 (1953) 336–339.
- [16] E. Orowan, in: G.M. Rassweiler, W.L. Grube (Eds.), *Internal Stresses and Fatigue in Metals*, Elsevier, London, England, 1959.
- [17] M.D. Richards, C.J. Van Tyne, D.K. Matlock, *Mater. Sci. Eng. A* 528 (2011) 7926–7932.
- [18] D.V. Wilson, G.R. Ogram, *J. Iron Steel Inst.* 206 (1968) 911–920.
- [19] H.P. Tardif, C.S. Ball, *J. Iron Steel Inst.* 182 (1956) 9–19.
- [20] R.A. Elliot, E. Orowan, T. Udoguchi, A.S. Argon, *Mech. Mater.* 36 (2004) 1143–1153.
- [21] W.C. Jeong, *Metall. Mater. Trans. A* 29A (1998) 463–467.
- [22] M.W. Hukle, B.D. Newbury, D.B. Lillig, J. Regina, A.M. Horne, *Proc. of the ASME 27th Int. Conf. on Offshore Mech. and Arctic Eng.*, Paper No. OMAE2008-57874, Estoril, Portugal, June 15–20, 2008, pp. 457–470.
- [23] A. Liessem, J. Schroeder, M. Pant, M. Erdelen-Peppler, M. Liedtke, S. Hohler, C. Stallybrass, *New Developments on Metallurgy and Applications of High Strength Steels*, TMS, Buenos Aires, Argentina, May 26–28, 2008, pp. 543–555.
- [24] D.-M. Duan, J. Zhou, B. Rothwell, D. Taylor, K. Widenmaier, *Proc. of the 7th Int. Pipeline Conf.*, Paper No. 64426, Calgary, Alberta, Canada, September 29–October 3, 2008.
- [25] Y. Li, W. Zhang, S. Gong, L. Ji, C. Huo, Y. Feng, *Proc. of the 8th Int. Pipeline Conf.*, Paper No. 31180, Calgary, Alberta, Canada, September 27–October 1, 2010.
- [26] D.-M. Duan, J. Zhou, B. Rothwell, D. Horsley, N. Pussegoda, *Proc. of the 7th Int. Pipeline Conf.*, Paper No. 64427, Calgary, Alberta, Canada, September 29–October 3, 2008.
- [27] Y. Shinohara, T. Hara, E. Tsuru, H. Asahi, Y. Terada, N. Doi, *Proc. of the 24th Int. Conf. on Offshore Mech. and Arctic Eng.*, Halkidiki, Greece, June 12–17, 2005.
- [28] Y. Yutori, S. Nomura, I. Kokubo, H. Ishigaki, *Proceedings of the 11th IDDRG, Les Memoires Scientifiques Revue Metallurgie, Mars*, 1980, pp. 561–569.
- [29] J. Marzbanrad, *WSEAS Trans. Appl. Theor. Mech.* 6 (2007) 127–131.
- [30] G.P. Dicostranzo, D.K. Matlock, R.P. Foley, *SAE Technical Paper No. 960024*, 1996.
- [31] M.A. McCormick, J.R. Fekete, D.J. Meuleman, M.F. Shi, *SAE Technical Paper No. 980960*, 1998.
- [32] Y.-Y. Wang, M. Liu, *Proc. of the 8th Int. Pipeline Conf.*, Paper No. 31376, Calgary, Alberta, Canada, September 27–October 1, 2010.
- [33] Y.-Y. Wang, D. Horsley, M. Liu, *APIA Joint Technical Meeting*, Canberra, Australia, April 17–20, 2007, pp. 1–15.
- [34] M.L. Macia, S.A. Kibey, H. Arslan, F. Bardi, S.J. Ford, W.C. Kan, M.F. Cook, B. Newbury, *Proc. of the 8th Int. Pipeline Conf.*, Paper No. 31662, Calgary, Alberta, Canada, September 27–October 1, 2010.
- [35] *Europipe*. <http://www.europipe.com/files/production-overview-uo-e-gb.pdf> (3.1.2011).
- [36] J. Raffo, R.G. Toscano, L. Mantovano, E.N. Dvorkin, *Mecán. Comput.* XXVI (2007) 317–333.
- [37] C. Timms, L.O. Mantovano, H.A. Ernst, R.G. Toscano, D. Swanek, D. DeGeer, M.P. Souza, L.C. Chad, *Rio Pipeline Conf. and Exposition*, Paper No. IBP1382.09, Rio de Janeiro, Brazil, September 22–24, 2009.
- [38] P. Shewmon, *Diffusion in Solids*, 2nd edn, Wiley Publishing, Hoboken, NJ, USA, 1989.
- [39] C. Wert, *Phys. Rev.* 79 (1950) 601.
- [40] D.G. Crone, L.E. Collins, Y. Bian, P. Weber, *Proc. of the 8th Int. Pipeline Conf.*, Calgary, Alberta, Canada, September 27–October 1, 2010.
- [41] R. Klein, L.E. Collins, F. Hamad, X. Chen, D. Bai, *Proc. of the 8th Int. Pipeline Conf.*, Calgary, Alberta, Canada, September 27–October 1, 2010.